Journal of Luminescence 199 (2018) 334–338

Contents lists available at ScienceDirect

Journal of Luminescence

journal homepage: www.elsevier.com/locate/jlumin

Thermoluminescence study in $Cu_3Ga_5S_9$ single crystals: Application of heating rate and T_m–T_{stop} methods

M. Isik[a,*], N.M. Gasanly[b,c], L.G. Gasanova[d], A.Z. Mahammadov[d]

[a] Department of Electrical and Electronics Engineering, Atilim University, 06836 Ankara, Turkey
[b] Department of Physics, Middle East Technical University, 06800 Ankara, Turkey
[c] Virtual International Scientific Research Centre, Baku State University, 1148 Baku, Azerbaijan
[d] Department of Physics, Baku State University, 1148 Baku, Azerbaijan

ARTICLE INFO

Keywords:
Thermoluminescence
Trap distribution
T_m–T_{stop} method

ABSTRACT

$Cu_3Ga_5S_9$ semiconducting single crystals were investigated using thermoluminescence (TL) measurements in 10–300 K temperature region. In the TL glow curve, one peak starting to appear at the instant temperature is increased from 10 K and another peak, which is broader than a general individual TL peak, were observed. The broad peak around 66 K was investigated using T_m–T_{stop} experimental method to understand whether or not this peak is composed of more than one individual peaks or continuously distributed traps. Curve fitting, initial rise and peak shape methods were used for acceptable TL curves to be analyzed. TL curves in T_m–T_{stop} method indicated that observed peaks are due to the existence of quasi-continuous distribution of traps. Structural characterizations of $Cu_3Ga_5S_9$ single crystals were studied using x-ray diffraction and energy dispersive spectroscopy measurements. The crystal structure, lattice parameters and atomic composition of the elements were reported in the present paper.

1. Introduction

$Cu_3B_5C_9$ ternary semiconductors, where B = Ga or In and C = S, Se or Te, have potentials as photo-absorbers in solar cells, optoelectronics devices, and photoelectrochemical cells [1–5]. They are visible-light-active crystals with high-absorption coefficients and suitable band gaps [6–8]. The production probability of $Cu_3B_5C_9$-type semiconductors has been established based on the state diagram of $CuBC_2$–B_2C_3 systems [1]. $Cu_3Ga_5S_9$ compound is the representative of above-mentioned materials. The minute state diagrams of the $CuGaS_2$–Ga_2S_3 system has been investigated in Ref [9]. It has been found that at 25 mol% Ga_2S_3, the $Cu_3Ga_5S_9$ compound is formed with melting temperature of 1150 °C. The optical and electrical properties of $Cu_3Ga_5S_9$ crystals have been studied in Refs [10,11]. The room temperature energy band gap for the direct optical transitions was established as 1.88 eV. Eight active modes with frequencies of 150, 180, 233, 260, 310, 327, 362 and 387 cm^{-1} are detected in the infrared spectra [12]. The highest frequency band was attributed to the antiphase vibration of the trivalent cation and anion sublattices.

The influence of defects on the performance of optoelectronic devices is a well-known subject. In optoelectronic devices such as LEDs or lasers, defects may introduce non radiative recombination centers to diminish the internal quantum efficiency. In the case of electronic devices, defects introduce scattering centers lowering carrier mobility. Thus, it is very useful to get detailed information on energetic parameters of recombination and trapping centers in semiconductor in order to obtain high-quality devices.

Thermoluminescence (TL) is one of the most sensitive techniques that have been employed for the investigations of lattice imperfections [13,14]. TL is emitted as a result of recombination of thermally liberated trapped electrons with the trapped holes. Analysis of the TL below room temperature enables one to obtain information about shallow defects in the material even at very low defect concentrations. Our research group focuses on the investigations of shallow defects in binary, ternary and quaternary semiconducting crystals. Moreover, low temperature TL studies on different materials were reported previously by many researchers [15–19]. In this work, TL measurements giving opportunity to characterize the defect center(s) have been performed. TL properties of $Cu_3Ga_5S_9$ crystals have been investigated in the low temperature range of 10–300 K. The defect levels in $Cu_3Ga_5S_9$ single crystals were revealed by the help of the analysis of the observed TL spectra and the characteristics of these levels have been reported. Crystal structure and atomic composition ratio of the constituent elements in $Cu_3Ga_5S_9$ crystals were also reported.

* Corresponding author.
E-mail address: mehmet.isik@atilim.edu.tr (M. Isik).

https://doi.org/10.1016/j.jlumin.2018.03.076
Received 8 November 2017; Received in revised form 15 February 2018; Accepted 23 March 2018
Available online 26 March 2018

2. Experimental details

$Cu_3Ga_5S_9$ polycrystals were synthesized from high-purity elements taken in stoichiometric proportions. Copper (Fluka cat. no. 61,140), gallium (Aldrich cat. no. 263,273) and sulfur (Fluka cat. no. 84,680) were of 99.999% purity. Generally, the synthesis of binary and ternary chalcogenide compounds is accompanied by high pressure of the chalcogenide vapors. Therefore, a special method has been developed for the synthesis of compounds with high volatile components. $Cu_3Ga_5S_9$ single crystals were grown from synthesized polycrystals by the Bridgman method in evacuated (10^{-5} Torr) silica tubes. The ampoule was moved in a vertical furnace through a thermal gradient of 30 °C/cm, between 1180 and 880 °C at a rate of 1.0 mm/h.

The chemical composition of the crystals was determined using the energy dispersive spectroscopy (EDS) experiments which were performed by a JSM-6400 scanning electron microscope having two equipments called as “Noran System6 X-ray microanalysis system” and “Semafore Digitizer” which take part in the analysis of experimental data. The crystal structure properties were identified using x-ray diffraction (XRD) experiments. Measurements on the powder samples were performed using “Rigaku miniflex” diffractometer with CuKα radiation (λ = 0.154049 nm). The scanning speed of the diffractometer was 0.02°/s. Experiments were accomplished in the diffraction angle (2θ) range of 15–90°.

Thermoluminescence measurements, performed in a temperature range of 10–300 K by means of “Advanced Research Systems” closed cycle helium gas cooling cryostat, were accomplished by illuminating the sample at low temperatures using LED creating light at a maximum peak of 2.6 eV. The sample with dimensions of 11 × 10 × 4 mm^3 was illuminated for 300 s. Illuminated sample was left in dark for an expectation time (≈ 120 s) after the excitation was turned off and Lake-Shore 331 temperature controller was adjusted to increase the temperature of the sample with a constant heating rate. An optical system comprising lenses and mirrors was used to gather emitted photons which were focused on the photomultiplier tube (Hamamatsu R928; spectral response: 185–900 nm). Pulses from the photomultiplier were converted into TTL pulses using a photon-counting unit (Hamamatsu C3866) and counted by a counter (National instrument NI-USB 2011). Number of photon counts was obtained as a function of temperature using a software program written in LABVIEW (National Instruments) graphical development environment. Further details of the system can be seen in Ref [20].

3. Results and discussion

Fig. 1 shows the EDS spectrum of the studied sample to get the chemical composition of the crystal. The EDS analyses are based on the

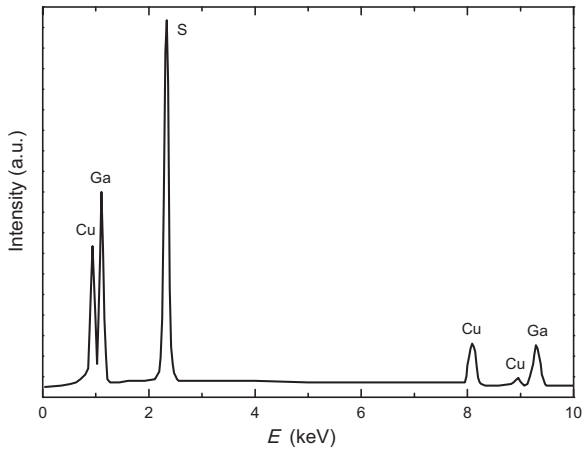

Fig. 1. Energy-dispersive spectroscopic analysis of $Cu_3Ga_5S_9$ crystal.

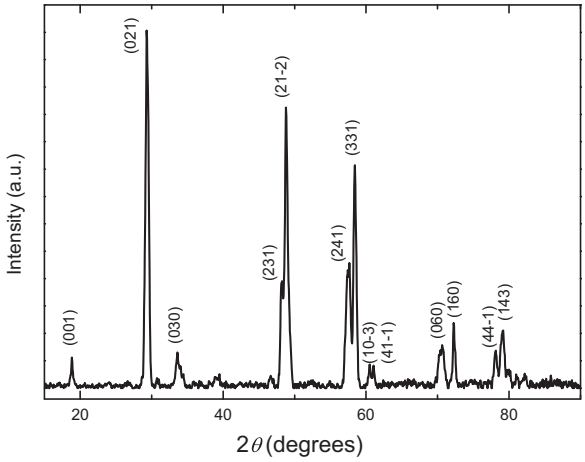

Fig. 2. X-ray powder diffraction pattern of $Cu_3Ga_5S_9$ crystal.

relative counts of the detected X-rays which are emitted from the radiated sample and characteristics for every element having unique energy levels [21]. The emission energies for Cu, Ga and S elements are (0.930, 0.933, 0.950, 0.953, 8.040, 8.904 and 8.961 keV), (1.098, 1.125, 1.144, 1.171 and 9.241 keV) and (0.163, 0.164, 2.307, 2.464 and 2.470 keV), respectively [22]. EDS measurements showed that the atomic compositions of the studied samples (Cu: Ga: S) was found to be 18.4: 29.8: 51.8.

XRD technique was used to obtain the structural parameters of the $Cu_3Ga_5S_9$ crystal. The crystal system, Miller indices of the diffraction peaks and lattice parameters were evaluated by means of least-squares computer program “DICVOL 04″. Fig. 2 shows the X-ray powder diffraction pattern of $Cu_3Ga_5S_9$. The sharp diffraction peaks are the indication of the well crystallinity of the sample. We picked out for indexing only the strong peaks with intensity $I / I_0 > 3\%$. The rest of diffraction peaks with intensities less than 3% are probably related with impurity phases in the studied sample. As illustrated in Table 1, the observed and calculated interplanar distances d are in agreement. The Miller indices (hkl) of the reflection planes are shown in Fig. 2 and also listed in Table 1. The lattice parameters of the monoclinic unit cell -were found to be $a = 0.4700$ nm, $b = 0.7995$ nm, $c = 0.6513$ nm, and $\beta = 90.79°$.

Fig. 3 presents the observed TL glow curves for $Cu_3Ga_5S_9$ crystal obtained at various heating rates changing between $\beta =$ 0.3 and 0.8 K/s. Our home-made experimental set-up has ability to perform the measurements in the temperature range of 10–300 K. Although we carried out the experiments at the starting point of measurements in this wide temperature range, outgoing experiments were done up to temperature value at which traps are completely emptied. As can been seen from the heating rate dependence TL curves, two peaks (A and B)

Table 1
X-ray powder diffraction data for $Cu_3Ga_5S_9$ crystal.

No.	$h\ k\ l$	d_{obs} (nm)	d_{calc} (nm)	I / I_0
1	0 0 1	0.4704	0.4700	8.6
2	0 2 1	0.3046	0.3045	100
3	0 3 0	0.2665	0.2665	9.8
4	2 3 1	0.1883	0.1883	29.9
5	2 1 − 2	0.1865	0.1865	78.4
6	2 4 1	0.1598	0.1598	35.0
7	3 3 1	0.1580	0.1579	62.3
8	1 0 − 3	0.1528	0.1528	6.6
9	4 1 − 1	0.1517	0.1517	6.3
10	0 6 0	0.1333	0.1333	12.0
11	1 6 0	0.1306	0.1306	18.2
12	4 4 − 1	0.1222	0.1222	10.5
13	1 4 3	0.1209	0.1209	16.1

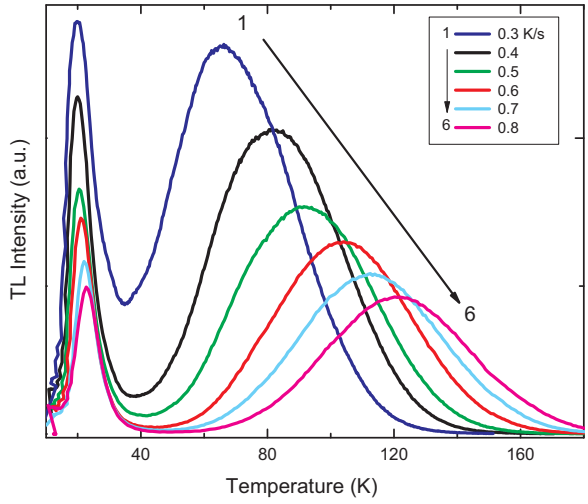

Fig. 3. Experimental TL curves of $Cu_3Ga_5S_9$ crystal with various heating rates.

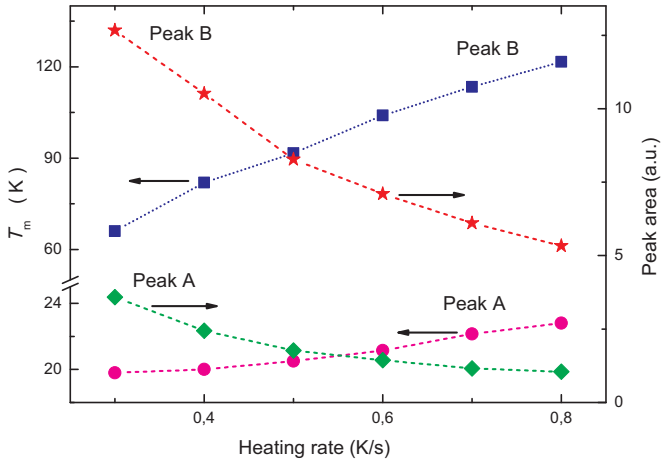

Fig. 4. The heating rates dependencies of the peak maximum temperature (T_m) and - areas of TL peaks.

were observed with maximum temperatures (T_m) shifting to higher temperatures from 19.9 to 22.8 K and from 65.8 to 121.9 K, respectively, by elevating the heating rates from 0.3 to 0.8 K/s. Dependencies of peak maximum temperatures (T_m) and peak areas were plotted for both peaks A and B as shown in the Fig. 4. As can be understood from the figure, peak maximum temperature shifts to higher values as expected according to theoretical expressions [13] and peak area decreases with increase of heating rate. The shift of the peak maximum temperature can be explained theoretically by the relation for the first order of kinetics as [13]

$$\beta = \nu \frac{kT_m^2}{E_t} \exp\left(-\frac{E_t}{kT_m}\right)$$

where E_t and ν symbolize activation energy and frequency factor, respectively. According to this equation, the increase of heating rate results in shift of peak maximum temperature to higher values. The shift of T_m with β was also explained empirically by Anishia et al. reporting TL responses of lithium magnesium borate (LMB) phosphors [23]. Authors' explanation is as follows: At a specific low heating rate β_1, the time spent by the phosphor at a temperature T_1 is long enough so that an amount of thermal release of charge carriers depending on half-life at T_1 could take place. For bigger heating rate of β_2, the time elapsed at the T_1 decreases and thus thermal release of trapped charge carriers also decreases. A higher temperature T_2 is needed to thermally release same amount of charges to take place at β_2. This results in shift of peak maximum to higher temperatures as heating rate increases in a manner depending on the half-life and time spent at each temperature. The decrease of peak area is an indication of the fact that the amount of charge carriers making radiative recombination decreases. This is the result of well-known effect called as thermal quenching which is the decrease of efficiency of luminescence due to the opening of non-radiative recombination centers as temperature is increased.

The observed glow curves can be analyzed to find activation energies of corresponding trapping centers. In the literature, there are many methods such curve fitting, initial rise and peak shape methods. At the beginning of analyses we have tried to apply curve fitting method which is based on the fitting of observed curve according to equations describing the temperature dependency of TL intensity. For this purpose, observed TL curve were tried to be fitted under the thought of that TL curve is composed of two individual peaks. Unfortunately, attempts were unsuccessful when all type of kinetics; first, second and mixed orders, were used. The reason of unsuccessful fitting process was understood due to presence of quasi-continuously distributed trapping centers as will be mentioned in the next paragraph.

Initial rise method is one of the powerful techniques used for all order of kinetics. In this method, initial portion of the TL curve is analyzed using the theoretical fact of that TL intensity (I_{TL}) in this region is proportional to $(-E_t / kT)$ [13]. The disadvantage part of this method is the point that obtained activation energy from the slope of I_{TL} vs. $1/T$ is related to trapping center emptying firstly. The activation energies of other trapping centers cannot be obtained from this method. When TL curve is carefully looked through, it can be detected that TL curve exist at the instant temperature is increased. Therefore, investigations of this portion for initial rise method do not give reliable results. Peak shape method takes advantage of temperature values of T_m, T_l and T_h which symbolize the peak maximum, low and high half intensity temperatures, respectively [13]. One requirement to apply this method is that these temperature values must be obtained from TL curve for individual peaks. Overlapping peaks damage this condition and cannot be analyzed using this method. In addition to activation energy calculation, this method also gives information about the order of kinetics responsible for TL transitions. Chen and Kirsh [24] predict the value of characteristic parameter $\mu_g = (T_h - T_m)/(T_h - T_l)$ to be between 0.42 (first-order kinetics) and 0.52 (second-order kinetics) for a single individual peak. The μ_g value for the peak B was found as 0.55 which is higher than the predicted range (Table 2). Since the recorded μ_g values are bigger than the theoretical limit, peak shape method cannot be applied on related TL glow curves. This value can be interpreted to existence of either more than one peak or quasi-continuous distribution of TL peaks within peak B. McKeever proposed a method to estimate the number and positions of individual peaks within a complicated TL curve [25]. This method, called in some papers as T_m–T_{stop}, is applied as follows [25–27]: Sample is illuminated at low temperature (T = 10 K for our measurements) and then heated at constant rate up to a temperature value (T_{stop}) at which some of the traps are emptied

Table 2
Activation energies (E_t) of measured TL glow curves and characteristic parameter (μ_g).

T_{stop} (K)	10	20	30	40	50	60	70
E_t (meV)	11 ± 1	20 ± 1	30 ± 2	60 ± 3	87 ± 4	121 ± 6	169 ± 8
μ_g	0.56 ± 0.02	0.55 ± 0.02	–[a]	0.74 ± 0.03	0.63 ± 0.03	0.63 ± 0.03	0.57 ± 0.03

[a] T_l and T_h values cannot be read in the related curve.

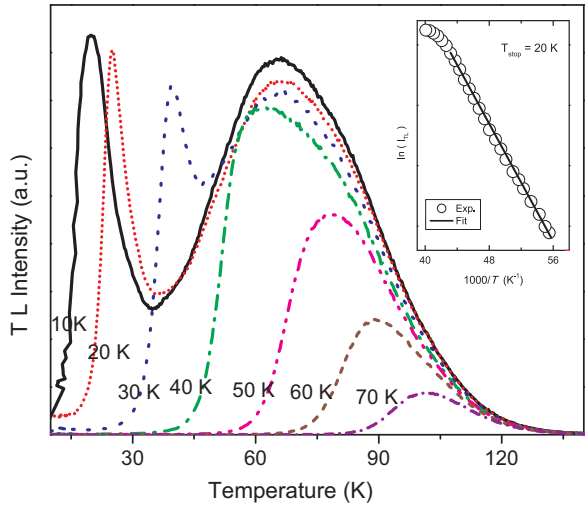

Fig. 5. The TL curves of $Cu_3Ga_5S_9$ crystal at various temperatures T_{stop} registered with heating rate 0.3 K/s. Inset shows the plot for initial rise method application on T_{stop} = 20 K curve.

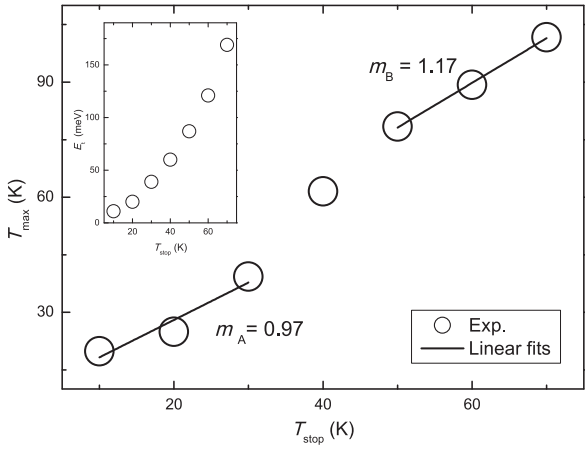

Fig. 6. T_m—T_{stop} plot for $Cu_3Ga_5S_9$ crystal. T_m values were read from the location of the first local maximum. Solid lines represent the linear fits. Inset: E_t—T_{stop} plot. E_t values were obtained from initial rise methods.

completely or partially. This T_{stop} value is generally chosen in the temperature range at which TL peaks started newly to be existence. The sample is cooled to initial low temperature and then TL measurements are carried out in all temperature range. Since some of the charges are excited from trap levels when sample temperature was stopped at T_{stop} temperature, new TL curve is formed due to remaining charge carriers. Fig. 5 shows the TL curves obtained for different stopping temperatures at constant heating rate of 0.3 K/s. In the T_m—T_{stop} method, stopping temperature dependency of first local peak maximum temperature is plotted. According to McKeever, if this curve has structure of "staircase", it means that there are well separated glow peaks having peak maximum temperature values corresponding to flat region. Another option is the existence of quasi-continuous distribution within one complex TL peak. In this case, T_m—T_{stop} plot presents a line with a slope of m~1.0. As can be seen from Fig. 6, observed TL peaks carries the properties of quasi-continuous distribution of traps. According to Fig. 5, first local peak maximum temperatures for peaks corresponding to stopping temperatures 10, 20 and 30 K -are related with peak A and 50, 60 and 70 K -are related with peak B. Therefore, linear fits of these different regions were performed separately. The slopes of these regions were obtained as m_A = 0.97 and m_B = 1.17 which are closer to reported slope of ~ 1.0 [25]. The activation energies of first emptying

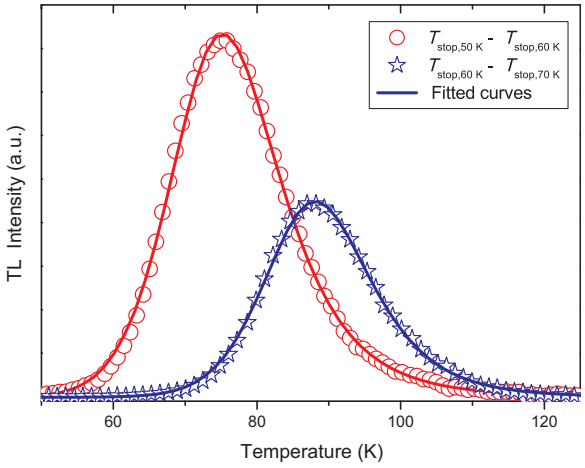

Fig. 7. Subtracted ($T_{stop,i}$ – $T_{stop,i+1}$) TL curves. Circles and stars show the experimental curves, solid lines are fitted curves.

traps responsible for TL curves recorded at different T_{stop} values were obtained from initial rise method. Inset of Fig. 5 shows one of the relevant plots (T_{stop} = 20 K) for initial rise method applications. Inset of Fig. 6 indicates the E_t—T_{stop} plot. Activation energies were found as increasing from 20 ± 1 meV (T_{stop} = 20 K) to 169 ± 8 meV (T_{stop} = 70 K) as presented in Table 2.

As a further analyses method on T_{stop} curves, we subtracted two sequential TL curves of 50–60 K and 60–70 K. As mentioned above, observed glow curves are responsible for quasi-continuously distributed trapping centers. By subtracting two sequential TL curves, we aimed to get TL curve associated for an individual peak. Fig. 7 shows the subtracted TL peaks (circles and stars). The analyses of these peaks were accomplished using curve fitting, initial rise and peaks shape methods. The solid lines in Fig. 7 are fitted curves under the light of second -order of kinetics. As can be seen, experimental subtracted and fitted curves are well matched. The outcomes of used software program indicated that activation energies of traps responsible for subtracted 50–60 K and 60–70 K curves are 83 ± 4 meV and 121 ± 6 meV (Table 3). The E_t values obtained from initial rise method applied to curves of stopping temperatures of 50 and 60 K were found as 87 ± 4 meV and 121 ± 6 meV. These closeness results indicate that subtracted curves are associated with individual peaks which are shallowest traps within the distributed traps. Initial rise and peak shape methods were also applied on these subtracted curves to obtain activation energies and characteristic parameters μ_g. The obtained results are given in Table 3. The calculated μ_g values also is a powerful indication of that second order of kinetics (fast retrapping) is the dominant mechanism for observed TL curves.

4. Conclusion

Characterization of trapping centers of $Cu_3Ga_5S_9$ single crystals were accomplished using low temperature thermoluminescence

Table 3
Activation energies (E_t) of subtracted TL glow curves and characteristic parameter (μ_g).

		E_t (meV)			μ_g
		Curve FittingMethod	InitialRise Method	Peak Shape Method	
$T_{stop,i}$ — $T_{stop,i+1}$ (K)	50–60 K	83 ± 4	89 ± 4	85 ± 4	0.52 ± 0.02
	60–70 K	121 ± 6	121 ± 6	128 ± 6	0.51 ± 0.02

experiments. TL spectra presented two peaks around 20 and 66 K. The applicability of some basic analyses techniques such curve fitting, initial rise and peak shape methods was not acceptable for observed peaks in TL curve. Heating rate dependence of TL curves was also investigated for studied crystal. The increase of heating rate resulted in decrease of TL intensity/area and increase of peak maximum temperature. The decrease of TL area with heating rate is the indication of thermal quenching effect. T_m—T_{stop} method was used to understand the behavior of TL characteristics of used crystal. Peak maximum temperatures of TL peaks were observed to be increasing as stopping temperature was increased. This behavior indicated the presence of quasi-continuous distributions of trapping centers.

References

[1] V.I. Tagirov, N.F. Gakhramanov, A.G. Guseinov, F.M. Aliev, G.G. Guseinov, A new class of ternary semiconductive compounds of type $A_3B_5C_9$, Sov. Phys. Crystallogr. 25 (1980) 237–239.

[2] T. Colakoglu, M. Parlak, Structural characterization of polycrystalline Ag-In-Se thin films deposited by e-beam technique, Appl. Surf. Sci. 254 (2008) 1569–1577.

[3] A. Guseinov, Cathodo- and Photoluminescence of $Cu_3Ga_5Se_9$ Single Crystals, Inorg. Mater. 47 (2011) 1049–1052.

[4] E. Guedez, L. Mogollon, G. Marcano, S.M. Wasim, G. Sanchez Perez, C. Rincon, Structural characterization and optical absorption spectrum of $Cu_3In_5Te_9$ ordered defect semiconducting compound, Mat. Lett. 186 (2017) 155–157.

[5] S. Ito, T. Ryo, Segregation of Cu-In-S elements in the spray-pyrolysis-deposited layer of CIS solar cells, Adv. Mater. Sci. Eng. 1 (2012) 136092.

[6] M. Gannouni, I. Ben Assaker, R. Chtourou, Influence of electrodeposition potential on the properties of $CuIn_5S_8$ spinel thin films, J. Electrochem. Soc. 160 (2013) H446–H451.

[7] N. Khemiri, M. Kanzari, Investigation on dispersive optical constants and electrical properties of $CuIn_5S_8$ thin films, Solid State Commun. 160 (2013) 32–36.

[8] A.G. Guseinov, A.G. Kyazimzade, V.M. Salmanov, R.M. Mamedov, A.A. Salmanova, L.G. Gasanova, A.Z. Mahammadov, Features of laser-induced luminescence and photoconductivity of layered $Cu_3In_5S_9$ crystals, Opt. Spectrosc. 121 (2016) 897–900.

[9] H. Ozkan, N. Gasanly, I. Yilmaz, A. Culfaz, V. Nagiev, Crystal data for $A_3B_5C_9$-type ternary compounds, Turk. J. Phys. 22 (1998) 519–524.

[10] V.I. Tagirov, N.F. Gakhramanov, A.G. Guseinov, K.M. Uk, Photoconductivity in $Cu_3Ga_5S_9$ single crystals, Sov. Phys. Semicond. 18 (1984) 1066–1067.

[11] V.I. Tagirov, A.G. Guseinov, N.F. Gakhramanov, K.M. Uk, Some physical properties of $Cu_3Ga_5S_9$ single crystals, Proc. Azerbaijan Acad. Sci. 4 (1984) 85–88.

[12] N.M. Gasanly, A.G. Guseinov, E.A. Aslanov, S.A. El-Hamid, Infrared reflection spectra of $Cu_3B_5C_9$ single crystals, Phys. Stat. Solidi (b) 158 (1990) K85–K88.

[13] R. Chen, S.W.S. McKeever, Theory of Thermoluminescence and Related Phenomena, World Scientific, Singapore, 1997.

[14] A.J.J. Bos, Theory of Thermoluminescence, Radiat. Meas. 41 (2006) S45–S56.

[15] J. Ji, L.A. Boatner, F.A. Selim, Donor characterization in ZnO by thermally stimulated luminescence, Appl. Phys. Lett. 105 (2014) 041102.

[16] D.T. Mackay, C.R. Varney, J. Buscher, F.A. Selim, Study of exciton dynamics in garnets by low temperature thermo-luminescence, J. Appl. Phys. 112 (2012) 023522.

[17] D. Winarski, C. Persson, F.A. Selim, Hydrogen in insulating oxide $Y_3Al_5O_{12}$ strongly narrows the band gap, Appl. Phys. Lett. 105 (2014) 221110.

[18] A. Anedda, C.M. Carbonaro, R. Carpino, M. Marceddu, O.B. Tagiev, A.N. Georgobiani, Low temperature thermoluminescence in $CaGa_2S_4:Eu^{2+}$, J. Lumin. 128 (2008) 1496–1500.

[19] T. Aitasalo, A. Durygin, J. Hölsa, M. Lastusaari, J. Niittykoski, A. Suchocki, Low temperature thermoluminescence properties of Eu^{2+} and R^{3+} doped $CaAl_2O_4$, J. Alloy Compd. 380 (2004) 4–8.

[20] M. Isik, E. Bulur, N.M. Gasanly, Low temperature thermoluminescence in $TlGaS_2$ layered single crystals, J. Lumin. 135 (2013) 60–65.

[21] J.J. Friel, X-ray and Image Analysis in Electron Microscopy, Princeton Gamma-Tech, Princeton, 2003.

[22] J. Goldstein, D. Newbury, D. Joy, C. Lyman, P. Echlin, E. Lifshin, L. Sawyer, J. Michael, Scanning Electron Microscopy and X-ray Microanalysis, Springer Science + Business Media, New York, 2007.

[23] S.R. Anishia, M.T. Jose, O. Annalakshmi, V. Ramasamy, Thermoluminescence properties of rare earth doped lithium magnesium borate phosphors, J. Lumin. 131 (2011) 2492–2498.

[24] R. Chen, Y. Kirsh, Analysis of Thermally Stimulated Processes, Pergamon Press, Oxford, 1981.

[25] S.W.S. McKeever, On the analysis of complex thermoluminescence glow-curves: resolution into individual peaks, Phys. Stat. Sol. (a) 62 (1980) 331–340.

[26] K. Brylew, W. Drozdowski, A.J. Wojtowicz, K. Kamada, A. Yoshikawa, Studies of low temperature thermoluminescence of GAGG:Ce and LuAG:Pr scintillator crystals using the T_{max}–T_{stop} method, J. Lumin. 154 (2014) 452–457.

[27] A.F. Soares, S.H. Tatumi, T.M. Mazzo, R.R. Rocca, L.C. Courrol, Study of morphological and luminescent properties (TL and OSL) of ZnO nanocrystals synthetized by coprecipitation method, J. Lumin. 186 (2017) 135–143.